



**HAL**  
open science

## Non-invasive local magnetic hysteresis characterization of a ferromagnetic laminated core

Sorelle Hilary Nguedjang Kouakeuo, Benjamin Ducharne, A. Solignac,  
Laurent Morel, Marie-Ange Raulet, B. Toutsop, Y. A. Tene Deffo, P. Tsafack

► **To cite this version:**

Sorelle Hilary Nguedjang Kouakeuo, Benjamin Ducharne, A. Solignac, Laurent Morel, Marie-Ange Raulet, et al.. Non-invasive local magnetic hysteresis characterization of a ferromagnetic laminated core. *Journal of Magnetism and Magnetic Materials*, 2021, 527, pp.167783. 10.1016/j.jmmm.2021.167783 . hal-03260454

**HAL Id: hal-03260454**

**<https://hal.science/hal-03260454>**

Submitted on 15 Jun 2021

**HAL** is a multi-disciplinary open access archive for the deposit and dissemination of scientific research documents, whether they are published or not. The documents may come from teaching and research institutions in France or abroad, or from public or private research centers.

L'archive ouverte pluridisciplinaire **HAL**, est destinée au dépôt et à la diffusion de documents scientifiques de niveau recherche, publiés ou non, émanant des établissements d'enseignement et de recherche français ou étrangers, des laboratoires publics ou privés.

# **Non-invasive local magnetic hysteresis characterization of a ferromagnetic laminated core.**

**S.H. Nguedjang Kouakeuo<sup>1,2,3</sup>, B. Ducharne<sup>2,4</sup>, A. Solignac<sup>5</sup>, L. Morel<sup>3</sup>, M.A. Raulet<sup>3</sup>, B. Toutsop<sup>1,2,3</sup>, Y.A. Tene Deffo<sup>1,2</sup>, P. Tsafack<sup>1</sup>.**

<sup>1</sup>Faculty of Engineering and Technology, University of Buea, Buea, Cameroon

<sup>2</sup>Laboratoire de Génie Electrique et Ferroélectricité, INSA de Lyon, 69100 Villeurbanne, France.

<sup>3</sup>Laboratoire Ampère, Université de Lyon, 69621 Villeurbanne, France

<sup>4</sup>ELyTMaX UMI 3757, CNRS – Université de Lyon – Tohoku University, International Joint Unit, Tohoku University, Sendai, Japan.

<sup>5</sup>SPEC, CEA, CNRS, Université Paris-Saclay, CEA Saclay 91191 Gif-sur-Yvette Cedex, France.

**Abstract:**

An alternative sensing solution is described to measure local magnetic hysteresis cycles through a laminated magnetic core. Due to the reduced space gap separating two successive laminations, it is impossible to interpose the usual oversize magnetic sensors (wound coil, Hall-effect sensor). In this study, the space issue has been solved by printing the needle probe method for the magnetic state monitoring and by using a micrometric Giant Magneto Resistance (GMR) for the magnetic excitation measurement. An instrumented magnetic lamination including the non-invasive monitoring solution has been built and moved successively to every lamination position of the whole laminated ferromagnetic core. A precise cartography of the hysteresis losses has been reconstructed from all these local measurements and the average values compared to the classic measurement methods obtained with a wound coil. The relative agreement between the experimental results observed opened doors to large improvement in the estimation of magnetic losses and in the design of magnetic circuits.

**Keywords:**

hysteresis characterization, needle probe method, micrometric giant magnetoresistance, printing technology, non-invasive sensor, local measurement.

## 1 - Introduction:

Electromagnets and electromagnetic conversions can be found in every industrial fields. They can be used as components or as electrical devices, such as motors, generators, transformers, loudspeakers, relays, inductors [1]-[3]. Once the magnetic field generated, a high permeability magnetic circuit drive the magnetic flux over the conversion area. This magnetic circuit has to be selected and dimensioned precisely since it is worth the main percentage of the conversion efficiency. For instance, when dealing with sensor-type applications where information has to be transmitted quickly, bulk ferrite materials are most of the time selected. Their weak macroscopic electrical conductivities, weak frequency dependences and high magnetic permeabilities give them strong advantages. Meanwhile, for power conversion applications purposes, like motors or transformers, ferromagnetic laminated cores are always preferred. Ferromagnetic laminated cores are constituted of stacks of thin electric steel laminations coated with an insulating layer, lying as much as possible parallel with the lines of flux. The layers of insulation serve as a barrier to the macroscopic eddy currents. Eddy currents can only flow in narrow loops within the thickness of each single lamination. Since the current in an eddy current loop is proportional to the area of the loop, this prevents most of the current from flowing, reducing eddy currents to a very small level. Since power dissipated is proportional to the square of the current, breaking a large core into narrow laminations reduces the power losses drastically. From this, it can be seen that the thinner the laminations, the lower the eddy current losses [4][5].

Improvements can also be obtained by increasing the magnetic lamination resistivity or by increasing the ferromagnetic lamination anisotropic behavior (grain-oriented (GO)) given that the magnetic excitation  $H$  and the magnetic induction  $B$  are collinear; thereby favoring conduction in the rolling direction.

In a ferromagnetic laminated core, the first lamination is set stuck to the second one, the second to the third one and so on. The coating layer ensures both the insulation and the adhesion of the laminations. This alternating structure (lamination, insulated layer ...) creates sometimes inhomogeneities in the magnetic stack which can be the source of local divergences in the magnetic behavior. Curvatures or undesired inclusions can also be sources of similar divergences.

For some years now, researchers from the electromagnetic numerical simulation domain have dedicated their time to generate simulation codes able to return the local behavior of laminated ferromagnetic core, homogenization methods were used [6]-[13]. These simulation methods were always validated by comparing these homogenized results with experimental measurements obtained with classic wound coils.

Space discretized methods were always chosen (finite elements, finite differences ...), these simulations give access to the local magnetic behavior of every single lamination. However, due to space restrictions these results have never been confronted to experimental ones. Unfortunately, it is impossible to insert in a non-intrusive way a classic magnetic measuring solution within the lamination stack.

In [14][15] authors have demonstrated the possibility to strongly reduce the size of the classic needle probe method by using solutions coming from the printed electronic domain. This elegant alternative method provides a magnetic state sensor of extremely reduced size ( $< 50 \mu\text{m}$ ) which can be inserted in the lamination stack without modifying its original structure. The idea of reduced thickness magnetic sensors for the characterization of magnetic laminated core is not new. In [16][17], by combining H-coils to the needle probe method authors reached a sensor of 2.7 mm total thickness. Scattering non-intrusive magnetic state sensors in the

magnetic core constitutes an innovative solution to detect undesired temperature hot-spots and to characterize local magnetic aging behaviors [18][19].

Now, if this Printed Magnetic Needle Probe (PMNP) gives access to the local magnetic induction field  $B$ , the local measurement of the magnetic excitation is still needed to get a complete information of the hysteresis cycle. In this new study, Giant Magneto-Resistance (GMR) sensor deposited on silicon wafer (thickness 270  $\mu\text{m}$ ) is positioned next to the PMNP sensor and used to monitor the excitation field  $H$  simultaneously. Even though the substrates' thickness in its original state is ten times higher than the printed sensor one, polishing treatments or adapted process of fabrication [20][21] can be performed to reduce the substrate thickness drastically ( $< 10 \mu\text{m}$ ).

The printed magnetic needle probe method (PMNPM) constitution and principles are reminded in the first section of this manuscript. The second part is dedicated to the GMR sensor description. The experimental setup developed for the validation of our local non-intrusive hysteresis cycle characterization is detailed in the third part. In the last section, comparisons between measurements will be proposed and we will recreate specific experimental conditions to generate a gradient of magnetic induction through the laminated magnetic core. We will monitor the local hysteresis cycle of every lamination and compare the sum of these local measurements to the average value obtained with a global wound coil.

## **2 - The printed magnetic needle probe method (PMNPM):**

### *2.1) The magnetic needle probe method: principles*

The needle probe method was first proposed by Werner [22] in 1949. It has however really been exploited at the end of the 20th century when large performance improvements in analog electronics allowed to isolate and amplified sufficiently the extremely weak

electromotive forces produced by this method [23]-[27]. By opposition to the destructive search coil method, the needle probe method is a non-destructive way to evaluate the local flux in a ferromagnetic lamination. According to [28], for measurements over distances greater than 10 mm any of the techniques can give accurate results. The local magnetic characteristics (magnetic state, permeability, etc.) of a ferromagnetic specimen can be evaluated using different method, Eddy Current Testing (ECT) [29], Magnetic Barkhausen Noise (MBN) [30][31], Magnetic Incremental Permeability (MIP) [32][33], but all these methods are affected by the bulkiness of the sensor design, which prevents for instance access to anisotropic magnetic behaviors. The needle probe method is a remarkable alternative to solve this directional issue, it is based on the application of two probe needles in contact with the specimen to be controlled and forms a half-cross sectional coil [34]. Based on the potential difference due to the eddy currents circulation when the specimen is submitted to an alternating excitation field, it becomes possible to evaluate the flux density in halved the cross-sectional area 1-2-3-4 as depicted in Fig. 1 below:

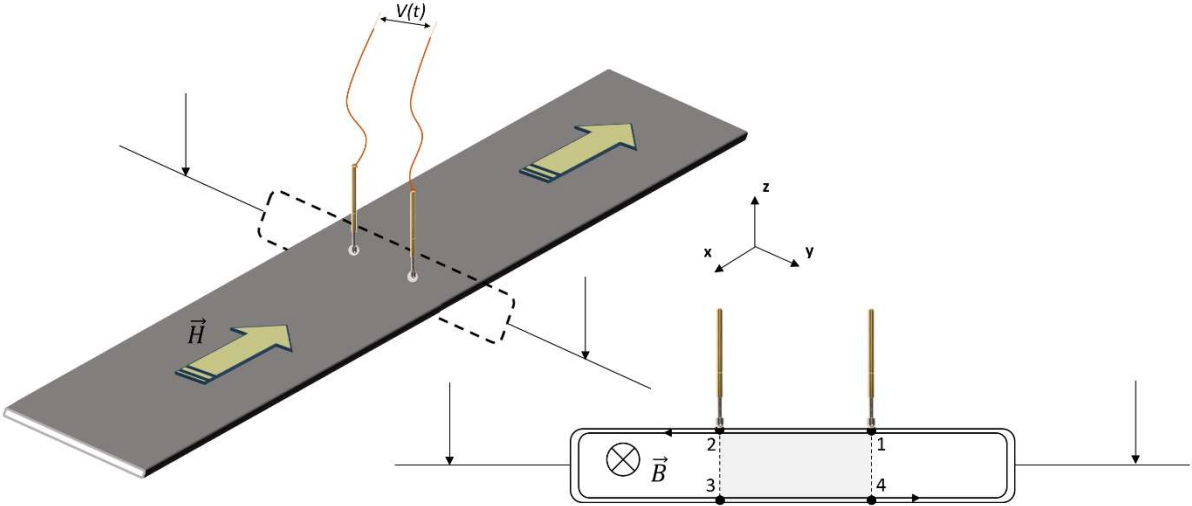


Fig. 1 – Magnetic needle probe method, explanation scheme.

As described in detail in [14][15], the voltage drop between position 1 and 2 can be approximated to:

$$V_{12} \approx \frac{1}{2} \int_{S_{1234}} \frac{\partial \bar{B}_{1234}}{\partial t} \cdot d\bar{S}_{1234} \quad (1)$$

Where  $V_{12}$  is the voltage drop between position 1 and 2.  $B_{1234}$  and  $S_{1234}$  are respectively the homogeneous magnetic field and the cross section through the position 1234 (Fig. 1). Eq. 1 approximation is particularly true far from the lamination edges. A

### *2.2) The Printed Magnetic Needle Probe (PMNP) method*

Printed Electronics (PE) is an all-encompassing term for the printing method used to create electronic devices by printing on a variety of substrates. Printed electronics technology has evolved over time, and now inkjet printers are capable of printing electrical circuits quite inexpensively and quickly. The rise of PE is mainly due to the development of new materials and in particular to a variety of Conductive Inks (CI) [35][36]. CI is defined as an ink that results in a printed object which conducts electricity. It is typically created by infusing graphite or other conductive materials (silver, copper, gold, etc.) into ink. In this work, a PE method is used to deposit a CI circuit on the surface of a ferromagnetic lamination and recreate the MNP method described in the previous section. For this, two options can be envisaged:

\_ The mask method:

A mask is used to expose areas representing the routes of the circuit and protect areas of the lamination from placement of trace material during the printing process. Since an electric steel lamination is electrically isolated, to ensure the electrical contact required by the PMNP, the insulating coating has to be scraped off locally before the printing process. Eventually, a soft fiber brush is used to deposit a fine layer of silver ink. Once the cure done, the mask is removed and the electrical circuit ready to use.

\_ The micro plotter printer method:

For this option, a high precision industrial printer is used. The Sonoplot printer (developed by the Sonoplot Company) consists of an automatic fluid dispenser (60 micron opening) and can deposit precisely layers of silver ink thinner than 30  $\mu\text{m}$ .

Results obtained with the A Keyence LJ-V7000 profilometer show thicknesses lower than 25  $\mu\text{m}$  for the micro plotter printed method and 28  $\mu\text{m}$  for the mask method. Additional descriptions such as images for both the printing methods can be find in [14][15].

### **3 - The giant magnetoresistive sensor**

The needle probe method in its printed version gives access in a non-intrusive way to the local and directional cross-section flux variation of a ferromagnetic lamination under dynamic external magnetic stimulus. After time-based integration and renormalization considering geometrical information,  $B(t)$  is obtained. Now to complete the plot of the corresponding hysteresis cycle as requested by the standard of characterization, the local tangent surface magnetic excitation  $H(t)$  has to be monitored as well.

#### *3.1) The giant magnetoresistive sensor: principles*

Giant magnetoresistive sensors exhibit a typical detection level of a few nanoteslas on a large frequency range [37][38]. They are composed of thin (< 10 nm) deposited layers on a thicker but still thin (270  $\mu\text{m}$ ) substrate which can be polished in post processing or thinned during the GMR fabrication [20][21]. The resulting overall GMR sensor on substrate thickness can drop to less than 1  $\mu\text{m}$ . Good detectivity and dispersion combined to possibly sub-micrometric dimensions make GMR sensors the best candidates for our  $H(t)$  measurement.

Giant MagnetoResistive (GMR) sensors are basically composed of two ferromagnetic layers separated by a metallic non-magnetic spacer. The first magnetic layer known as the reference layer is set in a well-defined magnetized state, which will be the sensitive sensor direction,

whereas the second layer magnetization is free to rotate under the influence of the external magnetic field. This rotation induces a resistance variation due to the spin-dependent charge transport [37][38]. The linearity of the resistance as a function of the magnetic excitation is made possible through a weak shape anisotropy (pinning of the free layer) created at 90° from the reference layer magnetization. This pinning shows furthermore the interesting property to reduce some undesired magnetic noise by magnetization stabilization and to control the field linearity range but it also reduced the sensor sensitivity [32]. The GMR we use in this study has the following structure: Si/ SiO<sub>2</sub> (500)//Ta (3)/Ni<sub>80</sub>Fe<sub>20</sub> (6.3)/Co<sub>90</sub>Fe<sub>10</sub> (2.1)/Cu (2.9)/Co<sub>90</sub>Fe<sub>10</sub> (2)/Ru (0.85)/Co<sub>90</sub>Fe<sub>10</sub> (2)/Ir<sub>22</sub>Mn<sub>78</sub> (7.5)/Ru (0.4)/Ta (5) (thicknesses in nanometers) and has been deposited by sputtering (Rotaris – Singulus) on Si oxidized wafers. Standard UV lithography technics are then used to fabricate meander shaped GMR structures with metallic contacts [37] and large pads for easier connection with the printed silver contacts as depicted in the inset of Fig. 2 (a) . Left hand side of Fig. 2 below illustrates the GMR magneto-transport  $R(H)$  characteristic when an external field is applied along its sensitive direction. The linear central part correspond to the sensing part when the free layer rotates before saturation in the parallel/ antiparallel state of the free and reference layer magnetization (low/high resistance state). This measurement has been performed by measuring with 2 probes the sensor DC output voltage in a home-made set-up. The magnetic excitation field was slowly varied along the reference layer direction through a Helmholtz coil between +/- 12 000 A/m. The noise spectral density was also measured and allowed extracting the sensitivity and the limit of detection, typically respectively 0.7 %/mT and 50 nT at 10Hz [32].

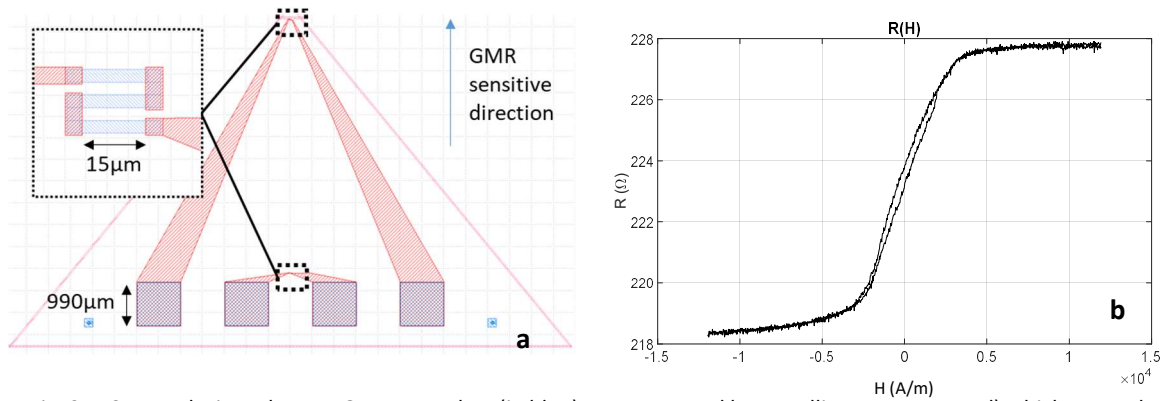


Fig. 2a –Sensor design. The two GMR meanders (in blue) are connected by metallic connections (red) which are ended by large pads to facilitate the connection. 2b – Typical,  $R(H)$  resistance response to an applied along the reference magnetization

### 3.2) The instrumented ferromagnetic lamination

The GMR substrate is then cut with a diamond saw in a triangular shape. The active part is the GMR located close to the contacts (Fig. 3, below). Analogous to the PMNP, a mask method is used to design the electrical circuits between the GMR pads and the external connections. The GMR substrate is stuck to the lamination and the active direction is set collinear to the ferromagnetic lamination rolling direction (see Fig. 3a). A special care has been taken to passivate the Si wafer side with insulating glue in order to avoid electric short-circuits in between contacts.

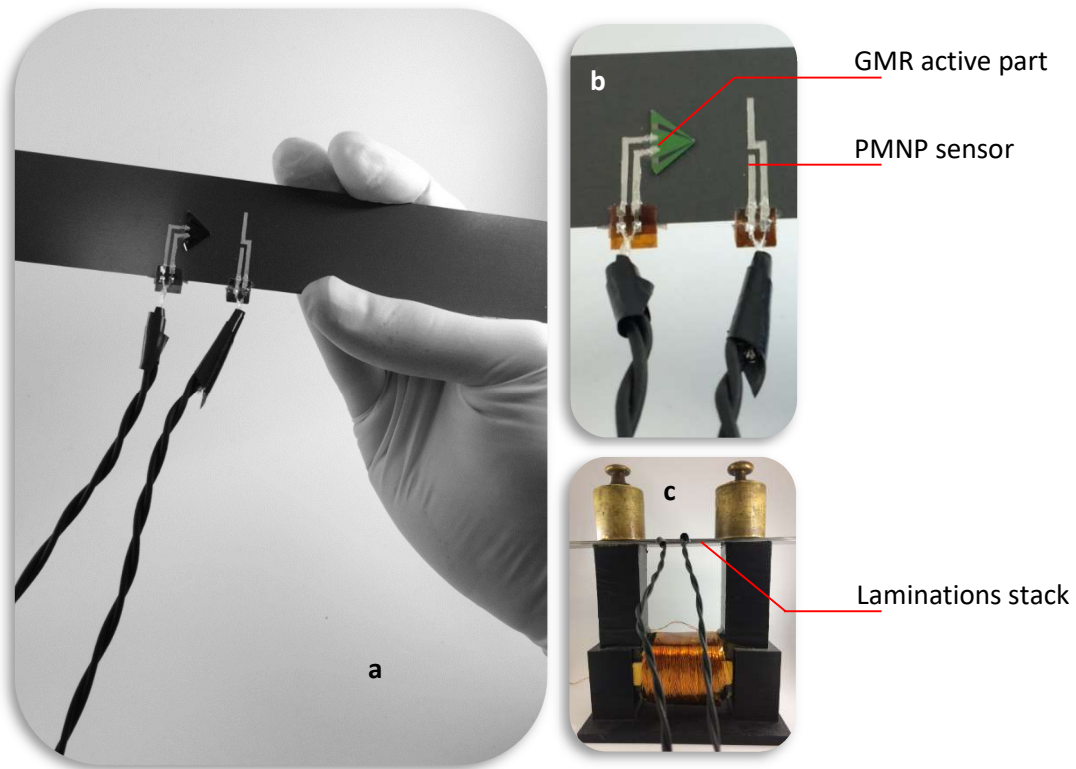


Fig. 3a – The instrumented ferromagnetic lamination, 3b – The non-invasive sensor, 3c – The sensor embedded in a lamination stack.

#### 4 – Experimental characterization setup

A dedicated experimental setup has been developed to validate the feasibility of our non-invasive local hysteresis cycle characterization method. Fig. 4 below depicts a 3D overview of this experimental setup.

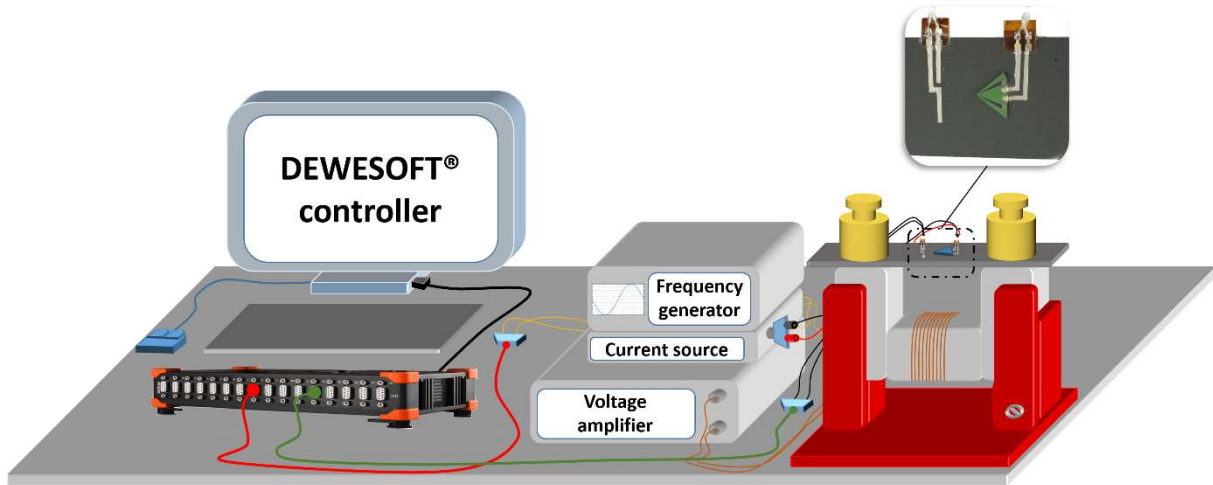


Fig. 4 –Overall 3D view of the experimental setup.

It is constituted mainly of a U-shape yoke of large cross-section (37 x 36 mm) and Fe-Si oriented grains laminated magnetic core. The weights on top of the lamination stack were made out of non-ferromagnetic brass. They ensured the mechanical stability. Based on the large permeability difference with the tested specimens, they were supposed of no influence on our experimental results. A 500 turns excitation coil was wound over the yoke as illustrated in Fig. 3c. A power amplifier Kepco BOP 100-4M in a controlled current configuration amplifies signal emanating from the frequency generator Agilent 32220A. The Kepco amplifier as the energy source, supplied the excitation coil. A current source built with analogue devices supplied the GMR with a current whose a controlled amplitude could vary from 1 to 3 mA. The data-acquisition of both the printed needle probe and the GMR sensor was ensured from the DEWESoftX2 data acquisition software associated to a SIRIUSif 8xCAN data acquisition system. The numerical integration and the drift correction of the PMNP signal was performed in a post-processing stage with MATLAB (R) software. A demagnetization of the tested specimens was completed before everynew acquisition. For this demagnetization process the same experimental setup was used, a 50 Hz sinus waveform of slowly decreasing

amplitude was imposed to the excitation coil. Two minutes are necessary to reach a complete demagnetized state.

### 5 – Experimental results

The experimental setup described in the previous section was used for all the experimental results recorded in this section. The pre-characterization (Fig. 2) of the GMR sensor was used to determine its sensitivity (voltage to field conversion ratio) to 0.7%/mT. The distance between both the electrical contacts of the PMNP sensor and the tested lamination thickness were respectively 10 mm and 0.35 mm. These geometrical information were used to convert the integrated signal into the magnetic field *B*. All tested specimens came from the same batch and were all oriented grain (GO) FeSi laminations with a 3wt% silicon content. Tab. 1 below provides the physical properties measured at room temperature for the FeSi GO as given by the manufacturer.

Tab. 1 – Typical values of FeSi GO basic magnetic parameters at room temperature.

Composition	Max. relative permeability ( $\mu_{max}$ )	Coercive field He (A/m)	Saturation polarization Js(T)	Curie Temperature Tc (°C)	Saturation magnetostriction $\lambda_s=(\Delta l/l)_{Js}$	
						GO Fe-Si
Core loss (W/kg)						
	W10/50	W10/400	W10/1k	W5/2k	W1/10k	W0.5/20k
GO FeSi	0.7	14.4	62.0	50.2	38.0	33.0

W10/50 is the core loss à 50Hz, 1T (10kGauss)

Before indulging into the core of our experiment, there is need of doing a characterization of the material been used. Through this characterization a crosscheck of the actual behavior will be compared to that described by the manufacturer. Thus, for the first experimental results displayed in Fig. 5, the instrumented lamination was laid on the single sheet tester and the magnetic excitation amplitude was gradually changing from 20 to 600 A/m.

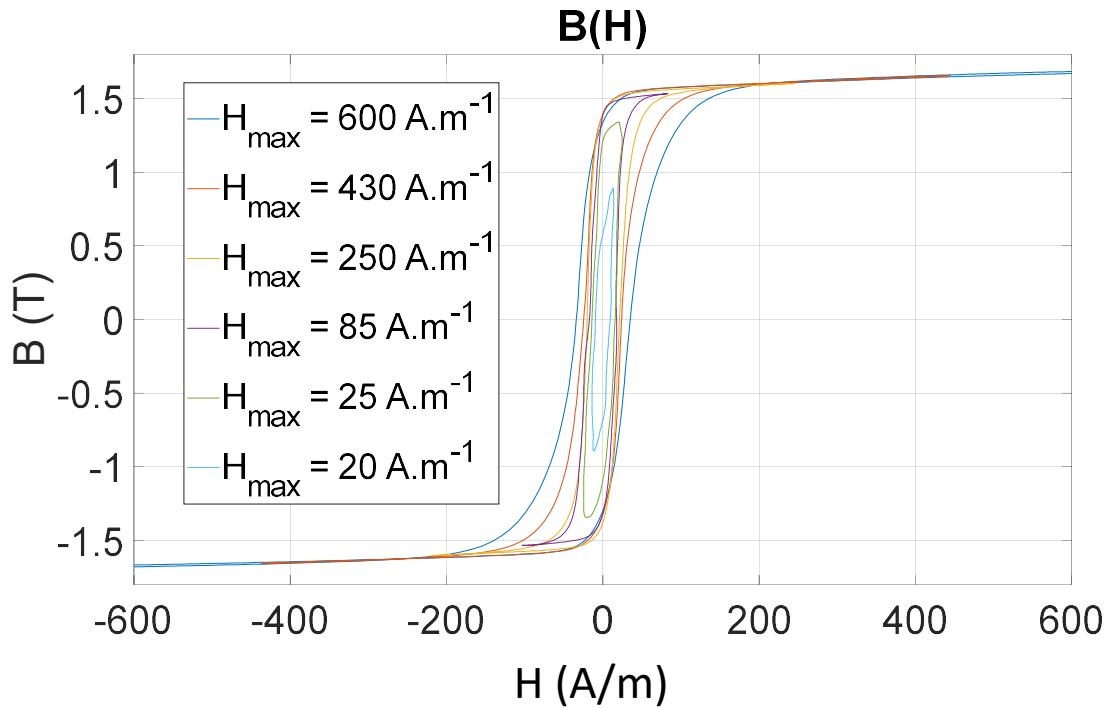


Fig. 5 – Experimental centered B(H) hysteresis cycles .

The first set of experimental tests was in good agreement with the authors expectations. The coercivity remained below 30 A/m and the induction saturation close to 1.8 T which is consistent with the scientific literature and the manufacturer information (Tab. 1). The cohesion in the behaviors reveals at an effectiveness of the GMR sensor used in measuring the magnetic field intensity.

The whole lamination stack was used for the next experimental test to mimic the environment similar to that of laminated magnetic core. Here, the instrumented lamination was successively moved from the first position up to the last one. The current amplitude in the excitation coil was set to ensure the reach of a saturated state in the bottom lamination (directly in contact with the yoke of the single sheet tester) and an unsaturated one for the top lamination (opposite position). Our idea here was to intentionally create a gradient of

magnetic states through the laminated core and validate the accuracy of the non-invasive characterization method. The frequency was set to 50 Hz to match the Western Europe standard of electrical energy distribution. The sensors of the instrumented lamination were adjusted in the middle of the yoke legs to ensure collinearity between the induction field and the lamination rolling direction. A local hysteresis cycle was measured for every lamination and plotted in Fig. 6 below.

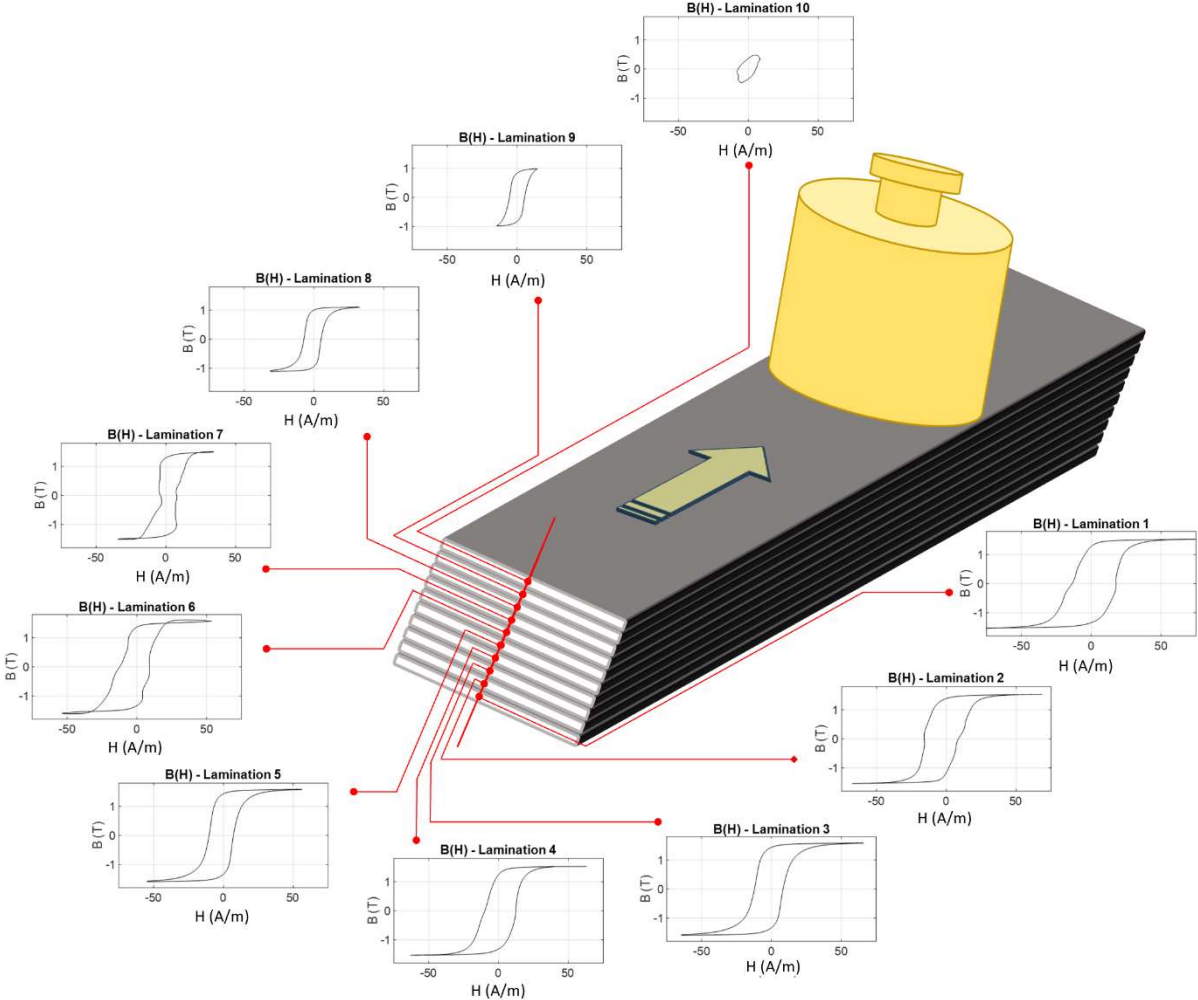


Fig. 6 – Local hysteresis cycles of the ferromagnetic laminated core.

Unexpected asymmetrical B(H) loops were observed for lamination 1,2,6,7 and 10, probably due to undesired parasitic behaviors during the signals acquisition. The position dependence of the classic magnetic hysteresis characteristics (the coercivity, the remanent induction, the

hysteresis area and the relative permeability) measured on the experimental results depicted in Fig. 6 are shown in Fig. 7 below:

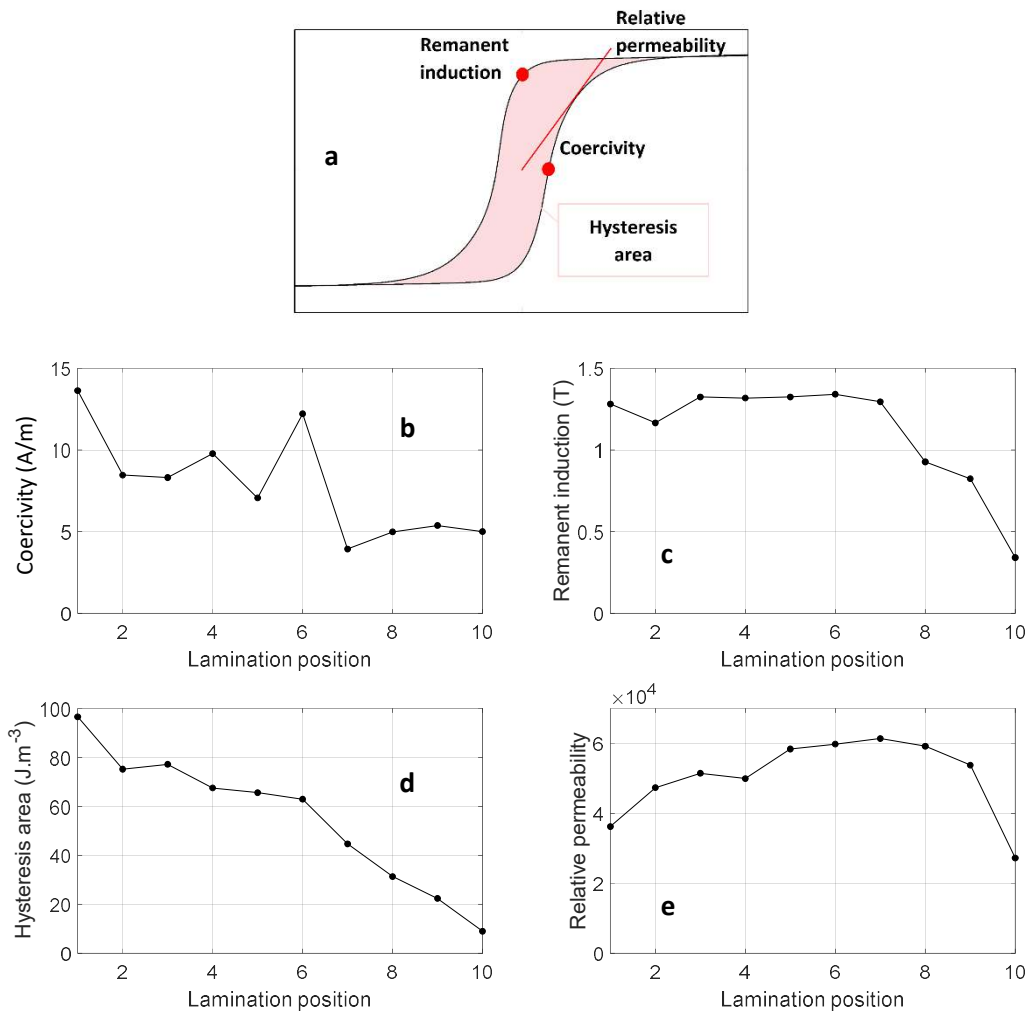


Fig. 7a – The hysteresis cycle parameters, 3b – Evolution of the coercivity as a function of the lamination position, 3c – Evolution of the remanent induction as a function of the lamination position, 3d – Evolution of the hysteresis area as a function of the lamination position, 3e – Evolution of the relative permeability as a function of the lamination position.

The variations of the classic hysteresis characteristics plotted in Fig. 7 (quasi linear reduction of the coercivity and of the hysteresis area, non-linear reduction of the remanent induction and conservation of the relative permeability as a function of the lamination position) are consistent with our expectations and confirmed the inhomogeneity of the laminations magnetic state. As a final validation step of the non-invasive characterization method, a 10

turns pick-up coil was wound all over the lamination stack. The electromotive force measured by this coil during the magnetization process was integrated and the drift corrected in post-processing just like we did for the PMNP sensor. This measurement returned the lamination stack average induction and was compared to the algebraic sum obtained considering the local measurements and the conservation of the magnetic flux:

$$\begin{aligned}\phi_{tot} &= \sum_{i=1}^{10} \phi_i \\ B_{tot} \cdot S_{tot} &= \sum_{i=1}^{10} B_i \cdot S_i \quad S_{tot} = 10 \cdot S_i \\ B_{tot} &= \frac{1}{10} \sum_{i=1}^{10} B_i\end{aligned}\tag{2}$$

Moreover, a Hall-effect sensor is used to evaluate the magnetic field intensity ( $H_{BOT}$ ) flowing in the lamination directly in contact with the yoke. The magnetic field  $H$  measured by this sensor is controlled to ensure the reproducibility of the magnetic conditions for every test required by this experimental situation.  $H_{TOP}$  is measured when the instrumented lamination is positioned on the upper layer of the lamination stack.

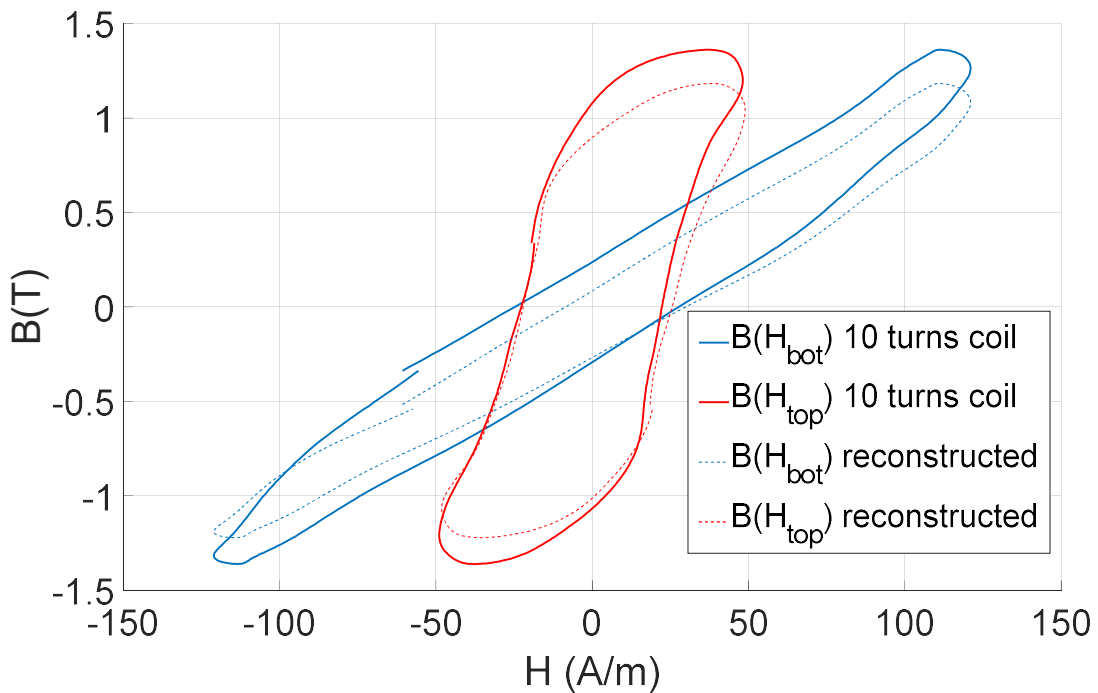


Fig. 8 – Comparisons between the reconstructed laminated hysteresis cycles and the measured ones.

Fig. 8 shows highly comparable results for both  $H_{BOT}$  and  $H_{TOP}$  reconstructed hysteresis cycles and experimental 10 turns coil cycles proving the validity of the non-intrusive sensors. The drift correction was adjusted on 5 period of acquisition. The small differences observable between the beginnings and the ends of the loops were due to small variations from one period of acquisition to another. These results provide evidence for the feasibility of monitoring isolated magnetic lamination states through the ferromagnetic laminated core. Concerning the surface areas, a 19 % and a 8 % relative deviation percentages (Eq. 3) can be calculated between the  $H_{BOT}(B)$  and  $H_{TOP}(B)$  hysteresis cycles respectively.

$$Relative\ deviation(\%) = 100 \cdot abs \left( \frac{reconstructed\ (H(B)_{area}) - wound\ coil\ (H(B)_{area})}{wound\ coil\ (H(B)_{area})} \right) \quad (3)$$

From these relative deviation evaluation, we can infer that, there is gain in precised information when dealing with GMR; thus portraying the validiting of using this method for the continuous monitoring of laminations in a magnetic core.

## 6 – Perspectives

Many perspectives can be envisaged for this work:

\_ In its current state, the characterization method was designed to ensure local measurement of  $\vec{B}$  and  $\vec{H}$  in a collinear situation and along the rolling direction of the instrumented lamination. However, in many cases both the magnetic state and the magnetic excitation directions vary from the rolling one (curvatures ...). A precise identification of these vector quantities could be done by coupling two set of sensors (Fig. 9 below): the first positioned in the rolling direction, the second in the transverse one. Vectors  $\vec{B}$  and  $\vec{H}$  can be returned through simple vector sum:

$$\begin{cases} \vec{B} = \vec{B}_{RD} + \vec{B}_{TD} \\ \vec{H} = \vec{H}_{RD} + \vec{H}_{TD} \end{cases}$$

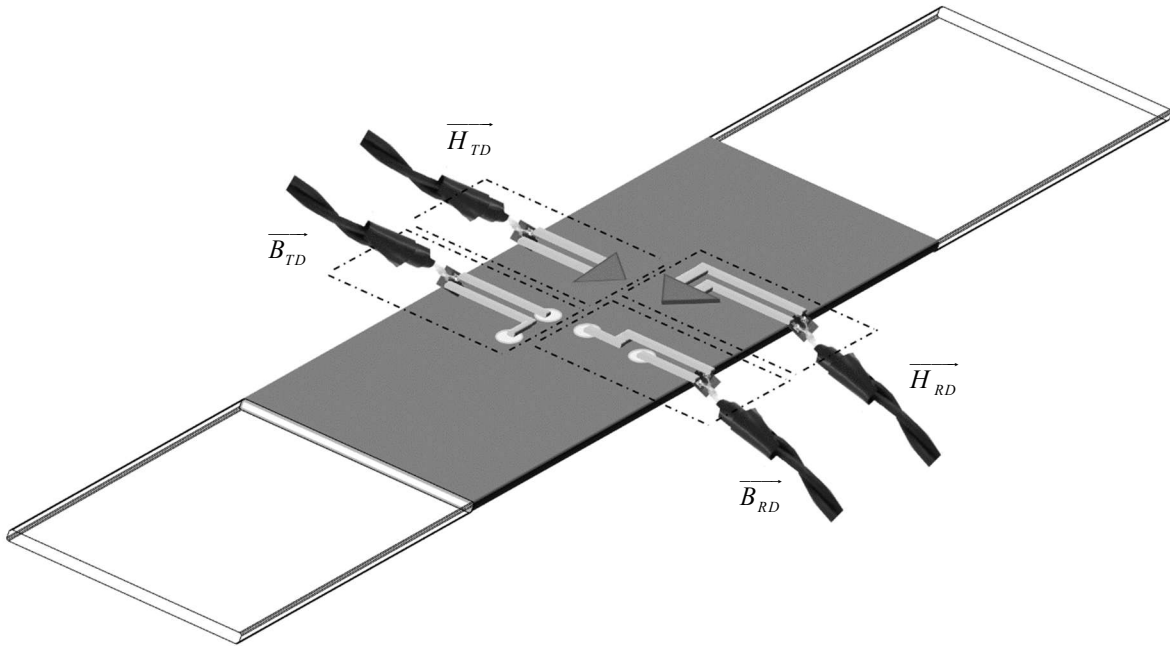


Fig. 9 – 2D experimental characterization configuration.

This non-invasive collect of magnetic directional data is also of high interest in the magnetic non-destructive testing domain where many times inaccessible parts have to be controlled and sensors as stealthy and compact as possible. Creep degradation and structural health monitoring are clearly targeted.

– Eventually, the comparison to simulation results constitutes another perspective of this study. In the introduction of the manuscript we claimed that many research work were dedicated to design simulation tools able to provide the magnetic behavior of an isolated lamination in the whole ferromagnetic laminated core. Now that our non-invasive sensor opens access to such experimental information, it would be of large interest to confront the simulation results to the experimental ones and validate the physical fundamentals used to develop the simulation methods.

## 7 – Conclusion

Ferromagnetic laminated cores are used systematically when large amount of energy are converted from an electrical form to a mechanical one. Even though the efficiency of those conversions is high, the strong non-linearity and frequency dependence of the ferromagnetic materials coupled to the irregularities in their geometries can be the source of magnetic inhomogeneities and local hotspots causing unexpected degradations. Since decades, industrials of this field have been developing simulation tools to anticipate the local behavior of ferromagnetic laminated cores but experimental validations were always limited to average quantities measured from surrounding sensors. In this manuscript, a whole non-invasive characterization method is proposed to measure the local hysteresis cycles through the laminated ferromagnetic core. An instrumented lamination has been built and moved successively to every position of the lamination pile. Printed methods derived from the printed electronic domain were used to design the electric connections. PMNP were used for the magnetic state characterization and miniaturized GMR for the magnetic field excitation. Due to the GMR substrate, the resulting sensor exhibits a still relatively large thickness of approximately 270  $\mu\text{m}$ . However, a polishing stage or thinning fabrication steps can be envisaged before its implementation and should reduce this thickness to less than 10  $\mu\text{m}$ . The non-invasive characterization method has been tested by comparing the average behavior obtained from all the local measurements to the classic experimental results observed with usual external techniques. Top and bottom measurement of the surface magnetic field were realized. Standard deviations lower than 20 % have been obtained in both cases. The sensors thickness is probably a source of changes in the local magnetic flux distribution. By reducing it, we hope to reduce those undesired changes and to improve the overall accuracy.

## References

- [1] S. Fizek, M. Reisinger, S. Silbers, W. Amrhein, "An electromagnet model comprehending eddy current and end effects", 2015 IEEE 11th International Conference on Power Electronics and Drive Systems, 15483825, Sydney, 2020.
- [2] A.M. Pawlak, "Magnets in modern rotary actuators", IAS '95. Conference Record of the 1995 IEEE Industry Applications Conference Thirtieth IAS Annual Meeting, 5144762, Orlando, 1995.
- [3] A. Goldman, "Handbook of Modern Ferromagnetic Materials", MA, Norwell: Kluwer, 1999.
- [4] K. Muramatsu, T. Okitsu, H. Fujitsu, F. Shimano, "Method of nonlinear magnetic field analysis taking into account eddy current in laminated core", IEEE Trans. Magn., Vol. 40, Iss. 2, pp. 896 – 899, 2004.
- [5] K. Yamazaki, S. Tada, H. Mogi, Y. Mishima, C. Kaido, S. Kanao, K. Takahashi, K. Ide, K. Hattori, A. Nakahara, "Eddy current analysis considering lamination for stator core ends of turbine generator", IEEE Trans. Magn., Vol. 44, Iss. 6, pp. 1502 – 1505, 2008.
- [6] Y. Du, Z. Cheng, Z. Zhao, Y. Fan, L. Liu, J. Zhang, J. Wang, "Magnetic flux and iron loss modeling at laminated core joints in power transformers", IEEE Trans. on App. Supercond., Vol. 20, Iss. 3, pp. 1878 – 1882, 2010.
- [7] J. Gyselinck, P. Dular, "A time-domain homogenization technique for laminated iron cores in 3-D finite element models", IEEE Trans. Magn., Vol. 40, Iss. 2, pp. 856 – 859, 2004.
- [8] J. Gyselinck, R.V. Sabariego, P. Dular, "A nonlinear time-domain homogenization technique for laminated iron cores in three-dimensional finite-element models", IEEE Trans. Magn., Vol. 42, Iss. 4, pp. 763 – 766, 2006.
- [9] H. Muto, Y. Takahashi, S. Wakao, "Magnetic field analysis of laminated core by using homogenization method", J. of App. Phys 99, 08H807, 2006.
- [10] M. A. Raulet, B. Ducharne, J.P. Masson, and G. Bayada, "The magnetic field diffusion equation including dynamic hysteresis: a linear formulation of the problem", IEEE Trans. on Mag., vol. 40, n° 2, pp. 872 – 875, 2004.
- [11] B. Ducharne, Y.A. Tene Deffo, B. Zhang, G. Sebald, "Anomalous fractional diffusion equation for magnetic losses in a ferromagnetic lamination", European Physical Journal Plus 135(3), 2020. DOI: 10.1140/epjp/s13360-020-00330-x
- [12] M. Schöbinger, K. Hollaus, I. Tsukerman, "Nonasymptotic homogenization of laminated magnetic core", IEEE Trans. Magn., Vol. 56, Iss. 2, 7509504, 2020.
- [13] Y. Takahashi, S. Wakao, K. Fujiwara, S. Fujino, "Large-scale magnetic field analysis of laminated core by using the hybrid finite element and boundary element method combined with the fast multiple method", IEEE Trans. Magn., Vol. 43, Iss. 6, pp. 2971 – 2973, 2007.
- [14] B. Ducharne, Y.A Tene Deffo, P. Tsafack, S.H. Nguedjang Kouakeuo, "Directional Barkhausen noise magnetic measurement using the magnetic needle probe method", Journal of Magnetism and Magnetic Materials 519, 2020. DOI: 10.1016/j.jmmm.2020.167453

- [15] S.H. Nguedjang Kouakeuo; Y.A. Tene Deffo, B. Ducharne, L. Morel, M.A. Raulet, P. Tsafack, J.M. Garcia-Bravo, B. Newell, "Embedded printed magnetic needle probes sensor for the real-time control of the local induction state through a laminated magnetic core", *J. Magn. Magn. Mater.*, Vol. 505, 166767, 2020.
- [16] G. Krismanic, H. Pfützner, N. Baumgartinger, "A hand-help sensor for analyses of local distributions of magnetic field and losses, *J. Magn. Magn. Mater.*, pp. 720-722, 2020.
- [17] G. Krismanic, H. Pfützner, N. Baumgartinger, "On the practical relevance of rotational magnetization for power losses of transformer cores",
- [18] J. Patel, K. Parekh, R.V. Upaghyay, "Prevention of hot spot temperature in a distribution transformer using magnetic fluid as a coolant", *Int. J. of Them. Sci.*, vol. 103, pp. 35-40, 2016.
- [19] X. Liu, Y. Yang, F. Yang, A. Jadoon, "Numerical research on the losses characteristic and hot-spot temperature of laminated core joints in transformer", *App. Therm. Eng.*, vol. 110, pp. 49-61, 2017.
- [20] C. Chopin, J. Torrejon, A. Solignac, C. Fermon, P. Jendritza, P. Fries, M.Pannetier-Lecoeur, "Magnetoresistive sensor in two-dimension on a 25  $\mu\text{m}$  thick silicon substrate for in vivo neuronal measurements", *ACS Sensors*, 2020.
- [21] M. Gerken, A. Solignac, D. Momeni Pakdehi, A. Manzin, T. Weimann, K. Pierz, S. Sievers, H. W. Schumacher, "Traceably calibrated scanning hall probe microscopy at room temperature", *physics.ins-det*, arXiv:1910.12676, 2020.
- [22] E. Werner, Austrian Patent n° 191015, 1949.
- [23] T. Yamaguchi, K. Senda, M. Ishida, K. Sato, A. Honda and T. Yamamoto, "Theoretical analysis of localized magnetic flux measurement by needle probe", *J. Phys. IV*, 8 717–20 Pr2, 1998.
- [24] K. Senda, M. Ishida, K. Sato, M. Komatsubara and T. Yamaguchi, "Localized magnetic properties in grain-oriented silicon steel measured by stylus probe method", *Trans. IEEE Jap.*, pp. 941–50, 1997.
- [25] K. Senda, M. Ishida, K. Sato, M. Komatsubara and T. Yamaguchi, "Localized magnetic properties in grain-oriented electrical steel measured by needle probe method", *Electr. Eng. Japan*, vol. 126, pp. 942 – 949, 1999.
- [26] K. Matsubara, T. Nakata, and Y. Kadota, "A novel method of measurements of magnetic flux in silicon steel sheet with magnetic flux leakage", in *National Conf IEE Japan*, 1665, 1988.
- [27] M. Enokizono and I. Tanabe, "The problem of simplified two dimensional magnetic measurement apparatus", in *5th International Workshop on 1 and 2-Dimensional Magnetic Measurement and Testing*, 1999.
- [28] G. Loisos, A.J. Moses, "Critical evaluation and limitations of localized flux density measurements in electric steels", *IEEE Trans. Magn.*, Vol. 37, NO. 4, pp. 2755 – 2757, 2001.
- [29] J. Garcia-Martin, J. Gomez-Gil, E. Vasquez-Sanchez, "Non-destructive techniques based on eddy current testing", *Sensors*, vol. 11, iss. 3, pp. 2525-2565, 2011.
- [30] B. Ducharne, B. Gupta, Y. Hebrard, J. B. Coudert, "Phenomenological model of Barkhausen noise under mechanical and magnetic excitations", *IEEE Trans. Magn.*, vol. 99, pp. 1-6, 2018.

- [31] B. Ducharne, MQ. Le, G. Sebald, PJ. Cottinet, D. Guyomar, Y. Hebrard, "Characterization and modeling of magnetic domain wall dynamics using reconstituted hysteresis loops from Barkhausen noise", *J. Magn. Magn. Mater.*, pp. 231-238, 2017.
- [32] B. Gupta, B. Ducharne, T. Uchimoto, G. Sebald, T. Miyazaki, T. Takagi, "Physical Interpretation of the Microstructure for aged 12 Cr-Mo-V-W Steel Creep Test Samples based on Simulation of Magnetic Incremental Permeability", *J. Magn. Magn. Mater.*, vol. 486, 2019.
- [33] B. Gupta, T. Uchimoto, B. Ducharne, G. Sebald, T. Miyazaki, T. Takagi, "Magnetic incremental permeability non-destructive evaluation of 12 Cr-Mo-W-V Steel creep test samples with varied ageing levels and thermal treatments", *NDT & E Int.*, Vol. 104, pp. 42-50, 2019.
- [34] Y.A. Tene Deffo, P. Tsafack, B. Ducharne, B. Gupta, A. Chazotte-Leconte, L. Morel, "Local measurement of peening-induced residual stresses on Iron Nickel material using needle probes technique", *IEEE Trans. Magn.*, Vol. 55, Iss. 7, 7100208, 2019.
- [35] J. Perelaer, P.J. Smith, D. Mager, D. Soltman, S.K. Volkman, V. Subramanian, J.G. Korvink, U.S. Schubert, "Printed electronics: the challenges involved in printing devices, interconnects, and contacts based on inorganic materials", *J. Mater. Chem.*, vol. 20, pp. 8446-8453, 2010.
- [36] B. K. Park, D. Kim, S. Jeong, J. Moon, J.S. Kim, "Direct writing of copper conductive patterns by ink-jet printing", *Thin solid films*, vol. 515, iss. 19, pp. 7706-7711, 2007.
- [37] J. Moulin, A. Doll, E. Paul, M. Pannetier-Lecoer, C. Fermon, N. Sergeeva-Chollet, A. Solignac, "Optimizing magnetoresistive sensor signal-to-noise via pinning field tuning", *Appl. Phys. Lett.* 115, 122406. 2019.
- [38] J. Torrejon, A. Solignac, C. Chopin, J. Moulin, A. Doll, E. Paul, C. Fermon, M. Pannetier-Lecoer, "Multi-GMR sensors controlled by additive dipolar coupling", *Phys. Rev. Applied* 13, 034031, 2020.